Comparison of Radio-Frequency-Plasma- and Ion-Beam-Induced Surface Modification of Kaolinite

Hui Ming,[†] Kaye M. Spark,[‡,§] and Roger St. C. Smart*[,†]

Ian Wark Research Institute, University of South Australia, Mawson Lakes, SA 5095, Australia, and CSIRO Land and Water, PMB 3, Griffith, NSW 2680, Australia

Received: August 13, 2000; In Final Form: January 30, 2001

Modification of the surface of kaolinite mineral particles was carried out in nitrogen, argon, helium, and air environments using the radio frequency (RF) plasma technique. The modified surfaces of the kaolinite were investigated by diffuse reflectance infrared Fourier transform spectroscopy (DRIFT) and X-ray photoelectron spectroscopy (XPS) to determine the surface speciation, the nature of the newly formed surface functional groups, and the interaction mechanism between the RF plasma and the kaolinite surface. Comparison with Ar^+ ion beam modification of kaolinite has established that the surfaces of kaolinite undergo low-energy ion bombardment with very limited sputtering in the presence of the Ar plasma but with no observable ion implantation. Surface restructuring with modified bonding is implied by this evidence. The steady-state charge behavior and surface structure of the kaolinite processed in the RF plasma showed significantly different characteristics from those of both the untreated kaolinite and an ion-beam-treated kaolinite. New infrared (IR) absorption bands were observed on the surfaces of RF-plasma-treated kaolinite at 1407, 2805, 3010, and 3100 cm^{-1}, along with some broad, partially resolved absorption bands which occurred near 1440 and 3280 cm^{-1}. The intensities of the newly formed IR bands were a function of the period of plasma treatment and the energy applied but were generally independent of the nature of the gas used for the plasma treatment. They are attributed to plasma-induced surface species arising from hydrocarbon contamination in the gas phase. In contrast to ion beam modification, the skeletal vibrations of the kaolinite lattice are not measurably affected in plasma treatments implying that restructuring, giving rise to the new IR bands, is confined to the surface layers.

Introduction

The surface modification of solid materials using plasmas is a dry, relatively fast and inexpensive technique. This technique involves high-energy electrons, ions, free radicals, excited molecules and atoms, generated in an electromagnetic field, striking the surface of a solid under vacuum. The effect of the interaction of these particles on the solid depends on the operating conditions (e.g., applied power, the nature and the pressure of the gaseous environment) and may include surface chemical reaction, sputtering, collision cascade, ion implantation, diffusion, local heating, lattice defect production, structural amorphization, and surface structure modification.[1−5] Most of these processes are associated with the surface monolayer (interface between solid and gas or vapour) or the near-surface region (region of physical penetration by the bombarding particles in which there is a collision cascade). Although the physical penetration of the plasma-induced particles is limited to the surface region, deeper regions may also be affected by local heating and diffusion.[2]

A radio frequency plasma is a non-equilibrium plasma in which the electron temperature, T_e, is far greater than that of the ion, T_i, (e.g., $T_e = 10^4-10^5$ K). The characteristics of RF plasmas include relatively low power application and low particle density (10^{8-13} particles/cm^3).[1,3−5] The energy of particles in a RF plasma process does not exceed 40 eV, and in most cases is less than 20 eV.[6] Because of this low ion energy, the field energy in a RF plasma process is delivered to the substrate in the form of bombarding ions promoting surface chemical interactions but relatively low heat generation at subsurface levels.[1] Recent studies have shown that even under very moderate RF plasma treatment, the surface damage to a substrate can be significant.[7−10] It has been found that ion bombardment resulting from RF plasma treatment not only changes the surface morphology of the impinged substrate, but also modifies other substrate surface properties, such as wettability and reactivity.[7−18] Other physical effects resulting from the ion bombardment including collision cascade, moderate local heat, and diffusion are often regarded as negligible for RF plasma treatment.

Kaolinite is one of the most abundant clay minerals. It has a general formula $Al_4Si_4O_{10}(OH)_8$ with a layered structure in which each layer consists of a siloxane tetrahedral sheet and a gibbsite-like octahedral sheet, and the individual layers are joined through hydrogen bonding.[19] The siloxane layer is regarded as relatively inert and the gibbsite layer and edge sites (i.e., SiOH, AlOH) exhibit weak acidic and basic properties.[18,20] As an important industrial mineral, kaolinite has been widely used in paper coating, ceramics, and fillers.[21,22] A previous study has shown that RF plasma modification can be successfully applied to increase the surface reactivity of kaolinite,[18] although the mechanism of such an interaction was not clearly identified. The interaction between RF plasma and kaolinite surface may be a complicated phenomenon perhaps involving a number of processes. Identification of the principal processes which have

* Author to whom correspondence should be addressed. Fax: 61 8 83023696. E-mail: Roger.Smart@unisa.edu.au.
[†] Ian Wark Research Institute, University of South Australia.
[‡] CSIRO Land and Water.
[§] Fax: 61 8 26960 1600. E-mail: Kaye.Spark@grf.clw.csiro.au.

10.1021/jp0031496 CCC: $20.00
Published on Web 03/31/2001

TABLE 1: XPS Analysis of Georgia Kaolinite (K) before and after Ar-Ion-Beam In-Situ Etching for Various Times

	atomic concentration (%)[a]			atomic ratio			static charge (eV)	binding energy (eV)[c]		
sample[d]	O	Si	Al	Si/Al	Si/O	Al/O		O1s	$Si2p_{3/2}$	Al2p
Ideal K	69.2	15.4	15.4	1	0.22	0.22				-
Georgia K[b]	70	16	14	1.15	0.23	0.20	4.4	532.1	102.9	74.5
10 min i.s.e.	65	17	18	0.94	0.26	0.27	5.2	531.6	102.3	74.5
30 min i.s.e.	66	15	19	0.78	0.22	0.29	5.2	531.5	102.3	74.5
120 min i.s.e.	66	16	18	0.90	0.24	0.27	6.7	531.6	102.1	74.6

[a] C1s at. % (<10%) due to hydrocarbon contamination removed. [b] as-received: impurities of N, Na, Ti: each <0.5 at. %. [c] Corrected by removal of static charge: referenced to C1s = 284.8 eV. [d] i.s.e.: in-situ Ar^+ etching.

a crucial effect on the surface properties of the kaolinite would enhance the possibility of effectively controlling and optimizing the plasma treatment to produce more specific changes. Furthermore, a clear understanding of the interaction mechanism associated with the plasma treatment of kaolinite may also assist in understanding the processes involved in using RF plasmas for the surface modification of any other similar materials, particularly clay minerals.

Experimental

Sample. Georgia kaolin, Hydrite, PX (Georgia) was purchased from the Georgia Kaolin Company. This commercial product is a well-ordered, water-processed kaolinite with characteristics of purity >97%, equivalent spherical diameter of >2 μm, median particle size of 0.7 μm, specific surface area (BET) 15.3 $\pm$ 0.5 m^2/g, giving a pH of 5 for a 0.1% aqueous slurry. The minor impurities present in the Georgia kaolin (from data supplied by the Georgia Kaolin Company), were Fe, Ti, Ca, Mg, Na, and K. The particles were cleaved, using grinding, to expose fresh surfaces, then water washed to remove any soluble impurities.

The chemicals used in this study were all A.R. grade. He, Ar, and N_2 were high purity gases from BOC Gases. Compressed and purified air was used for air plasma treatment.

Apparatus. The plasma reactor used in this study was a sealed large glass cylinder evacuated by a rotary pump to a vacuum of 10^{-3} torr, and was similar in design to instruments used in other studies.[12−18] A radio frequency electromotive force (emf) was applied to parallel copper bands (electrodes) attached to the outside of the glass reactor vessel. The kaolinite sample (2 g) was evenly spread on a glass plate, which was then placed in the middle of the reactor chamber between the copper electrodes. The standard operating conditions for the plasma treatment were the following: radio frequency 0.41 MHz, pressure 2×10^{-1} torr, and gas flow rate 4 standard cubic centimeters per minute (sccm). Power input was varied from 10 W to 50 W as described.

Diffuse reflectance Fourier transform infrared (DRIFT) spectra were recorded using a Nicolet Magna-IR 750 infrared spectrometer with a diffuse reflectance accessory (Spectra-Tech). The sample compartment of the instrument was continuously flushed with dry nitrogen to remove absorbed moisture and carbon dioxide. A KBr beam splitter and a liquid nitrogen cooled MCT/B detector were selected to analyze the samples. The DRIFT spectra were scanned between 400 to 4000 cm^{-1} at 25 °C in absorbance mode at 4 cm^{-1} resolution using 64 scans per sample. Dried KBr (Merck, spectroscopic grade) was used both to dilute the sample concentration to 5% by weight and as a background. The sample was allowed to equilibrate under the dry nitrogen in the sample compartment for 5 minutes before analysis to reduce the interferences associated with adsorbed water on the surface of the sample.

The surface composition of kaolinite was measured in a Perkin-Elmer PHI 5600 ESCA system using Mg Kα radiation at 300 W and 15 kV. The take-off angle was 45°, the pass energy was 95.94 eV, and the analyzed area of the sample was approximately 1 mm in diameter. The in-situ surface sputtering was conducted in the main chamber under Ar ion pressure maintained at 15 mtorr, with 3 kV ion energy using a sputtering area of 4×4 mm^2. The period of in-situ surface sputtering for all samples was 10 min at an etching rate of approximately 1 nm/min. All samples were first analyzed in the as-loaded form, followed by 10 min in-situ sputtering under Ar and then re-analyzed. The depth profile of the sample was conducted under similar conditions. The time interval for each surface sputtering prior to taking an XPS spectrum was 30 s. Ion beam treatment on kaolinite was also conducted in this system using similar operating conditions to those for in-situ sputtering, but with a sputtering area of 8×8 mm^2 and an etching rate of 0.25 nm/min. During an XPS measurement, the vacuum of the main chamber was maintained at 10^{-8} torr or less.

The kaolinite sample was prepared by applying a thick paste of kaolinite on a 8×8 mm^2 Pyrex plate, which was then dried at 70−80 °C. This preparation technique ensured that a dry film of kaolinite was attached well on the plate so that it could be easily transported to different apparatus (i.e., plasma, XPS analyses) for a variety of treatments and that the surface of the plasma-treated kaolinite analyzed by XPS was the same surface which had been directly affected by the RF plasma ions. The adventitious hydrocarbon on the surface of the sample was used as reference to correct for static charge on the kaolinite surface.[23,24] The uncharged binding energy (BE) of the contamination C1s line was 284.8 eV. All charge corrections and photoelectron peak resolutions, i.e., full width at half maximum (FWHM), were measured by computer analysis to eliminate possible errors associated with manual measurements. There is about 1% atomic concentration (at. %) Ar in all in-situ sputtered samples due to ion implantation. The concentration of Ar is not taken into account in calculating surface composition. Similarly, other impurities, either structural impurities or contaminants, are neglected in calculations in most cases.

Results

XPS Analysis of Georgia Kaolin. The results of the analysis of the surface composition of Georgia kaolin, investigated by XPS, are shown in Table 1. These indicate that the surface of the kaolinite was relatively clean except for hydrocarbon contamination. As this contamination was barely apparent (0.6 at. %) after in-situ etching (10 min) of the surface, it represents surface contamination only. The ratios of atomic concentrations of Si/Al, Si/O, and Al/O on the surface of the initial, as-received form of kaolinite were 1.15, 0.23, and 0.20, respectively, compared with the corresponding theoretical ratio values of 1.00, 0.22, and 0.22, respectively, derived from the stoichiometric

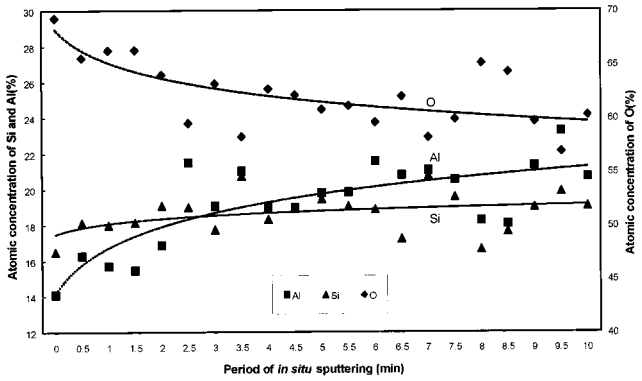

Figure 1. XPS atomic concentrations (%) from depth profiling of Georgia kaolinite by 3 kV Ar ions.

formula of kaolinite, $Al_4Si_4O_{10}(OH)_8$. After in-situ etching, the first ratio decreases to 0.94 while the other two increase to 0.26 and 0.28, respectively. A 0.8 eV increase in charge shift was observed on the etched sample, along with about 0.5 eV decrease in binding energy for all elements except Al which remained unchanged.

The effect on the atomic concentrations of Si, Al, and O in the Georgia kaolin as a function of sputtering time is shown in Figure 1. It recognized that the depth profiles are compromised by particles which are not in contact parallel to the plate surface but the results do indicate some selectivity. The 10 min of in-situ sputtering causes a gradual decrease in the relative concentration of O, an increase in that of Al, and little change in that of Si. The relative rates of sputtering for these three elements is therefore: rate of oxygen (R_O) > rate of silicon (R_{Si}) > rate of aluminum (R_{Al}). For a multi-component material, different rates of etching, i.e., preferential sputtering, of particular components, can result in a changing surface composition during sputtering until a steady state is reached.[25] In this case, the siloxane basal plane appears to be preferentially sputtered.

During sputtering, the concentrations of Si and Al (Figure 1) cross, resulting in a change in the Si/Al ratio from an initial value >1 to <1 after 3 min. As one basal layer of kaolinite is 7.15 Å thick,[19] the depth of sputtering (1 nm/min) after 3 min is equivalent to approximately 4 layers of kaolinite removed.

The apparent (uncorrected) binding energy (Figure 2) of three major elements showed a 0.6−1.75 eV shift to a higher binding energy (i.e., increased positive charge) during the 10 min of in-situ sputtering. While it is recognized that there is some scatter in the data, increases in both charge shifting and broadening of the XPS spectra were observed during the first 60 s of in-situ sputtering and changed little afterwards. For instance, the FWHM of O, Al, and Si increased from 2.1 to 3.3 eV, 2.0 to 2.6 eV, and 2.0 to 2.3 eV, respectively. These characteristics have been commonly observed in insulator materials.[25]

Plasma Treatment of Kaolinite. *(i) The Effect of Power Input.* The effect of plasma treatment on Georgia kaolin as a function of power input was determined using argon under the standard operating conditions described in the Experimental Section for a 3 h treatment time. As argon is an inert gas, the possibility of direct chemical interaction between the gaseous species and the surface of the kaolinite during plasma treatment is low.

There were no observed changes in the dominant characteristic IR peaks of kaolinite in the DRIFT spectra in the ranges 500−1300 cm^{-1} (skeletal vibration region of kaolinite molecule)

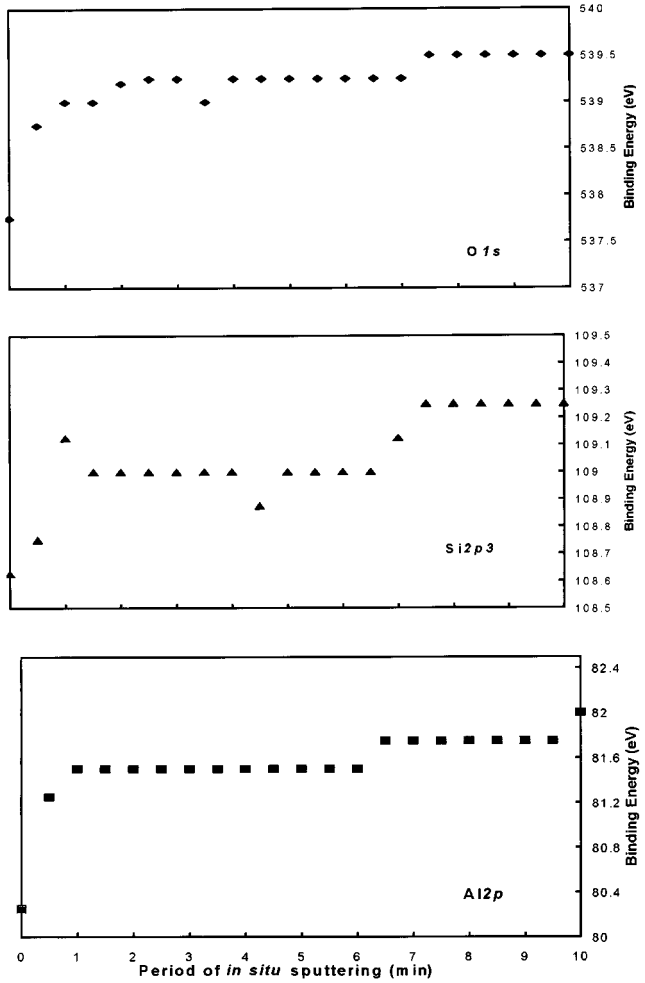

Figure 2. Variation of apparent binding energy of major element XPS signals during depth profiling of Georgia kaolinite.

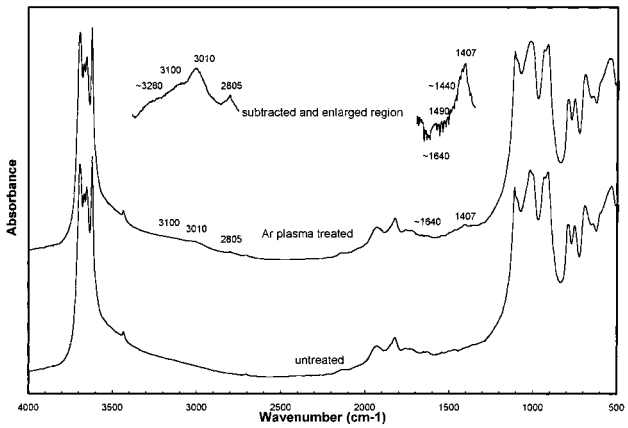

Figure 3. A comparison of the DRIFT spectra of Georgia kaolinite with and without Ar plasma treatment (50 W, 3 h) and their enlarged subtracted spectra.

and 3400−3800 cm^{-1} (OH functional group stretching vibration region) as a result of plasma treatment (Figure 3). Nevertheless, several new bands of relatively low intensity were apparent including those at 1407, 2805, 3010, and 3100 cm^{-1} illustrated in Figure 3. By subtracting the spectrum of a plasma-treated kaolinite from that of an untreated sample (Figure 3), several more plasma-induced weak IR bands are evident including two unresolved shoulders at ∼1440 cm^{-1} and ∼3280 cm^{-1}, as well as a small band at 1490 cm^{-1}. The plasma-induced bands near

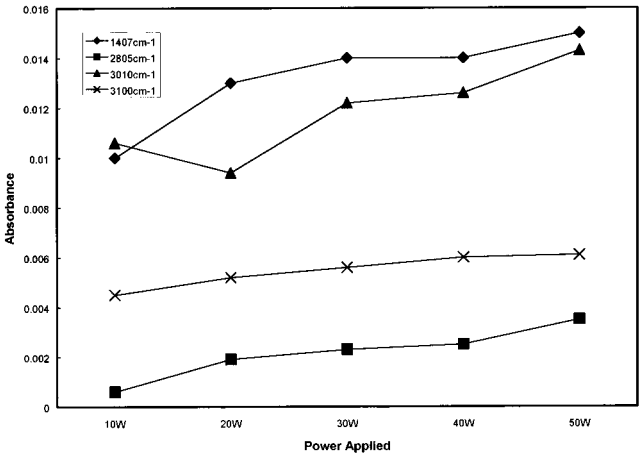

Figure 4. The intensity of newly formed FTIR bands on the surface of the kaolinite as a function of power applied during RF plasma treatment for 3 h.

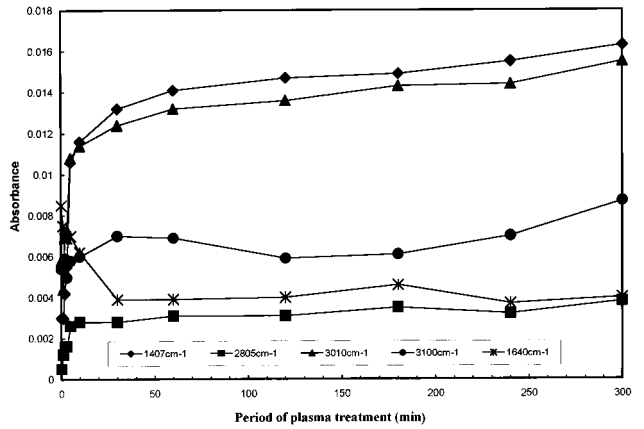

Figure 5. The variation of intensity of RF plasma (50 W)-induced IR bands as a function of the period of plasma treatment.

1407 cm^{-1} are small but relatively sharp, whereas the other four major bands at the higher wavenumbers are all rather broad. In addition, the IR band at 1640 cm^{-1} due to adsorbed water in the spectrum of the untreated kaolinite was reduced in the spectra of the plasma-treated kaolinite (which produced a negative feature in the subtracted spectrum in Figure 3).

The results in Figure 4 indicate that, under these experimental conditions, the intensity of the major plasma-induced IR bands increased slightly with increase in the power input of the plasma.

(ii) The Effect of Time. (a) RF Plasma Treatment. The effect of time on the plasma treatment of kaolinite was studied using the standard operating conditions and a fixed power input of 50 W. The DRIFT spectra of the samples treated for various periods of time, ranging from 1 min to 5 h, showed that the plasma-induced IR bands became significant at treatment times $\geq$2 min. Graphical representation (Figure 5) indicates that the intensities of the plasma-induced IR bands increase significantly during the first 10 min of plasma treatment, reaching >70% of the intensities observed after 5 h of treatment. In comparison, the intensity of the 1640 cm^{-1} band was reduced during the same 10 min period. As this band is attributed to the O−H bending vibration of adsorbed water, it is suggested that, as a result of plasma treatment, the adsorbed water may be either desorbed or forms a new adsorbed or reacted species.[26]

The atomic ratio Si/Al of the Georgia kaolin plasma treated for 0, 1, 2, 3, 5, 10, 30, 60, 120, 180, 240, and 300 min at 50 W was measured. Before the application of in-situ sputtering,

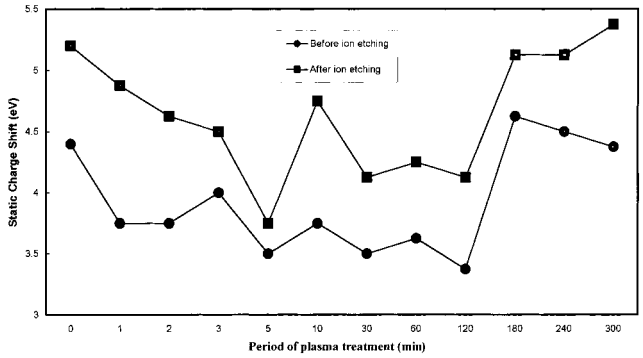

Figure 6. The effect of increased period of Ar plasma (50 W) treatment on the static charge shift before and after in-situ ion-beam sputtering (10 min) for Georgia kaolinite. Note the change of scale on the time axis.

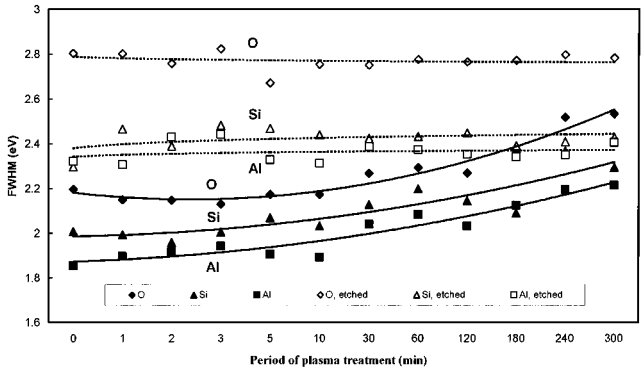

Figure 7. The full width at half maximum (FWHM) of O1s, Si2p, and Al2p XPS signals on the surface of Georgia kaolinite as a function of the period of Ar plasma treatment (50 W) before and after Ar-ion-beam (3 kV, 10 min) etching. Note the change of scale on the time axis.

the Si/Al ratio of plasma-treated samples tended to reduce with plasma treatment time from an initial value of 1.2 to 0.8 after 300 min of plasma treatment. For treatment times up to 120 min, the ratio was >1. The application of the in-situ XPS ion beam sputtering on the same plasma-treated Georgia kaolin samples took only 3 min to change the Si/Al ratio for all samples to <1. This result implies that surface sputtering on kaolinite during RF plasma treatment is very limited relative to that from in-situ sputtering.

For RF plasma treatment times not longer than 120 min, the charge shift on the surface of the as-received kaolinite (Figure 6), measured from the C1s spectra, tended to decrease with increase in plasma treatment time. Again, there is some experimental error producing scatter in the estimate of charge shift up to 120 min. However, plasma treatment times longer than 180 min resulted in considerable increase in charge shift (~1.25 eV) compared with shorter treatment times. The effect of the 10 min in-situ sputtering prior to plasma treatment was a general increase in charge shift of around 1 eV in all samples, again indicating more extensive sample damage.

Estimates of the peak widths of the O1s, Si2p, and Al2p signals for RF plasma-treated samples carry some uncertainty due to differing peak shapes and binding energy resolution. Nevertheless, the trends in Figure 7 showed very little change for plasma reaction times up to 10 min even though the intensity of plasma-induced IR bands underwent rather significant increases in the same period of time (Figure 5). However, over longer time periods up to 300 min of plasma treatment there was a gradual increase in the width of photoelectron peak

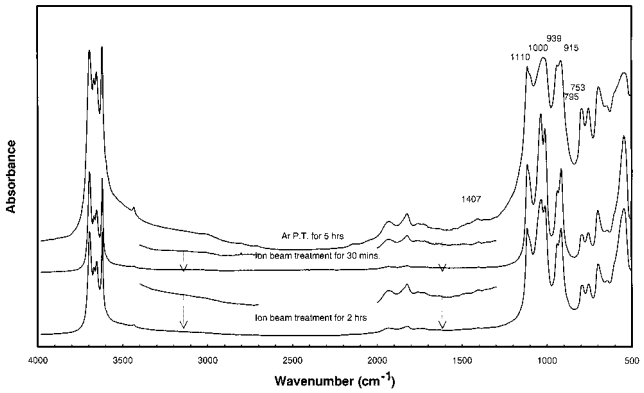

Figure 8. A comparison of DRIFT spectra of Ar plasma-treated (50 W, 5 h) with Ar ion beam-treated Georgia kaolinite (3 kV, 0.5 and 2 h).

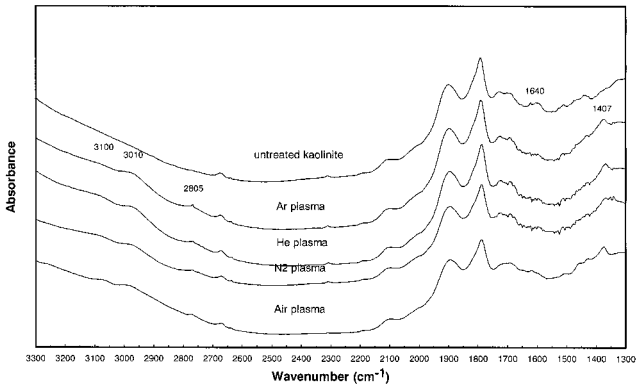

Figure 9. DRIFT spectra of plasma (50 W, 3 h)-treated Georgia kaolinite in various gases.

accelerating after 60−120 min. In contrast, the FWHM values of these samples after 10 min of in-situ sputtering prior to plasma treatment were significantly greater than those of the unsputtered samples and relatively constant regardless of the period of plasma treatment. This result tends to confirm the relatively limited surface sputtering effect of the plasma treatment under 60−120 min duration.

(b) Ion Beam In-Situ Surface Sputtering. The above experimental results confirm that RF plasma treatment of this magnitude involves both surface bombardment and restricted surface sputtering.[1−5] The intensities of RF plasma-induced IR bands on the kaolinite were increased as a function of time and energy applied (Figures 4 and 5). In order to examine the relationship between surface bombardment, surface sputtering, and the newly-formed IR bands, more intensive surface treatment of kaolinite using ion beam surface sputtering was conducted in the XPS main chamber.

The intensities of IR bands (e.g., 1407 cm^{-1}) associated with the surface of the kaolinite after prolonged in-situ sputtering of 30 min and 2 h, were similar in magnitude to each other (Figure 8) but were markedly reduced from those of the sample RF plasma treated for similar periods of time (e.g., Figure 3, 3h; Figure 8, 5h). In fact, the relative intensities of newly formed bands on both ion-beam-treated samples is even less than that of a sample treated in RF plasma for 10 min. Newly formed IR bands in the 2700−3300 cm^{-1} region are barely visible even after subtraction and enlargement. Furthermore, the intensities of some characteristic kaolinite IR bands were substantially reduced after ion-beam treatment. These bands include O−H deformation bands at 939 and 915 cm^{-1}, Si−O stretching vibration at 1110 cm^{-1}, and Si−O−Al stretching vibrations at 795 and 753 cm^{-1}. The split bands at 1000 and 1022 cm^{-1}, which are assigned to Al−O−Si and Si−O−Si stretching vibrations, respectively, are basically invisible in DRIFT spectra of the kaolinite with or without RF plasma treatment. As all of these changes in the IR spectrum appear below 1200 cm^{-1} in the skeletal vibration region, it appears that the surface structure of the ion-beam-treated kaolinite has been substantially altered. This indicates that the interaction between the high-energy ion beam and the surface of the kaolinite is much greater, as it principally affects the bonds associated with the bulk (and surface) structure of the kaolinite.

The XPS analysis of the surface of these kaolinite samples which had been subjected to prolonged in-situ Ar^+ ion beam sputtering is summarized in Table 1. Further development of the preferential sputtering observed for sputtering times of 10 min (Figure 1) is not apparent for these prolonged sputtering times, indicating that a steady state of sputtering has been reached.[25] In fact, the corrected binding energies of major components of the kaolinites sputtered for periods ≥10 min were very close in value. However, static charge shift on the surface of kaolinite ion beam treated for 2 h is higher than that for the other samples apparently due to positive charging associated with implantation of Ar^+ ions and/or surface damage.

About 1 at. % Ar was detected in all samples after XPS ion-beam in-situ sputtering. In contrast, no Ar was found on the surfaces of any of the plasma-treated kaolinite, even after 5 h of treatment. This indicates that the Ar ions generated in the RF plasma process are not sufficiently energetic to penetrate, or be implanted, in the kaolinite surface lattice as occurs in the in-situ ion beam process. These Ar ions, however, are apparently capable of restructuring atoms and bonding in the surface lattice of the kaolinite with very limited surface sputtering also observed.

(iii) Effect of the Nature of the Plasma Gas. The effect of the nature of the plasma ions on the RF plasma treatment of kaolinite was investigated using standard operating conditions, namely 50 kW of input energy and 3 h of treatment time. The gases used were He (inert but lighter than Ar), N_2 (more reactive than Ar), and dry air. The plasma treatments for 3 h with each gas were followed by 10 min in-situ Ar ion beam etching. These plasmas all induced a range of new IR bands (and reduction of the band at 1640 cm^{-1}) similar to those observed using the argon plasma (Fig. 9), although the intensities varied slightly depending on the nature of the gas being used. The XPS analysis of the surface of the kaolinite samples treated with these plasma gases is shown in Table 2. Unlike kaolinite Ar plasma treated for 3 h , the Si/Al ratio of all non-argon plasma-treated samples in the same treatment time is above 1. This may imply that sputtering preference of Si (and also perhaps Al) on kaolinite in non-argon gas plasma is different from that occurring when using the Ar plasma. As the mass of Ar is heavier than those of the other gases employed for plasma treatment, it is expected that the sputtering power of Ar under the same condition is more effective. It is noted that after 10 min of in-situ Ar sputtering for these non-Ar-plasma-treated samples, the Si/Al ratio was also reduced to less than 1.

No ion implantation was visible on the surface of any RF-plasma-treated samples confirming the interpretation that the energy of plasma-generated ions is too low for penetration or extensive sputtering. The binding energies and FWHM of all plasma-treated kaolinite showed only slight variations even in the case of relatively reactive gases such as nitrogen and air (Table 2). These results confirm that, under these experimental conditions, the type of gas used for generating the plasma has

TABLE 2: XPS Results from Georgia Kaolinite after Various Plasma and Plasma/Ion Etch Treatments

	atomic concentration (%)			atomic ratio			static charge (eV)	binding energy (eV)[a]			FWHM (eV)		
sample[b]	O	Si	Al	Si/Al	Si/O	Al/O		O1s	Si2p$_3$	Al2p	O1s	Si2p$_3$	Al2p
Ar plasma (3 h)	69	15	16	0.91	0.21	0.23	4.6	532.5	103.1	74.8	2.4	2.1	2.1
Ar plasma (3 h) + 10 min i.s.e.	66	17	18	0.93	0.25	0.27	5.1	531.8	102.4	74.5	2.8	2.4	2.3
He plasma (3 h)	67	18	15	1.25	0.23	0.22	4.3	532.7	102.8	74.5	2.6	2.4	2.3
He plasma (3 h) + 10 min i.s.e.	66	17	17	0.99	0.25	0.25	5.2	531.6	102.4	74.7	2.9	2.5	2.3
N_2 plasma (3 h)	69	16	15	1.14	0.23	0.21	3.7	532.4	103.1	74.8	2.3	2.2	1.9
N_2 plasma (3 h) + 10 min i.s.e.	65	17	18	0.93	0.26	0.28	4.7	531.8	102.3	74.4	2.8	2.5	2.3
air plasma (3 h)	68	17	15	1.16	0.25	0.21	4.0	532.4	103.3	74.8	2.3	2.0	2.0
air plasma (3 h) + 10 min i.s.e.	64	17	19	0.86	0.26	0.31	4.8	531.8	102.5	74.8	2.8	2.5	2.4

[a] binding energies charge corrected. [b] i.s.e.: in-situ Ar etching.

little effect on the formation of plasma-induced surface functional groups detected by DRIFT.

Discussion

Surface Structure of Kaolinite. The XPS analysis of the surface of the Georgia kaolin showed a Si/Al ratio greater than 1 for the initial sample and all plasma-treated samples (including gases other than argon) except those subjected to Ar plasma for longer than 2 h. The Si/Al ratio on the initial surface varied from 1.02 to 1.3 with the median at 1.15. Kaolinite is a dioctahedral phyllo-aluminosilicate so that the measured Si/Al ratio should be equal to 1.0. The Georgia kaolinite used is well crystallized; it would not be expected to contain silica as impurities in the surface layers. In this work, the kaolinite was initially applied to the glass plate as a thick paste and it would be expected that there would be random orientation of the crystal to the surface of the dried kaolinite film, and hence the proportion of gibbsite to silica faces presented to the X-ray should be approximately equal. The sampling depth (i.e., 3 × inelastic mean free path) during XPS measurement is a function of the kinetic energy of the element. For Si 2p and Al 2p signals in kaolinite, this sampling depth is roughly equal to 7 basal layers of kaolinite.[27]

One possible explanation for the high Si/Al ratio is that the outer basal faces of the Georgia kaolin are not an ideal kaolinite crystal as is generally assumed for a 1:1 alumino-silicate. A previous study has found that many naturally occurring kaolinite crystals contain pyrophyllite-like outer layers or smectite-like outer layers.[28] These non-ideal kaolinite outer layer structures are composed of two siloxane layers sandwiching a gibbsite-like layer in the middle. Existence of this type of non-kaolinite structure has been explained as the product of weathering processes during the transition of smectite to kaolinite.[28,29] The water and other cation concentrations during the weathering process may also play an important role in determining the type of outer layer formed.[30,31] The existence of this non-kaolinite outer basal layer in kaolinite would result in a high Si/Al ratio as measured by the surface-sensitive XPS technique.

The results from studies on surface charge characteristics of kaolinite have provided further evidence to support the XPS analysis.[32−34] It is generally accepted that the siloxane basal plane of the kaolinite carries a permanent negative charge.[35,36] The origin of the negative charge has been attributed to several possibilities including isomorphous substitution of Si^{4+} by Al^{3+}, other impurities with net negative charge, a silica-rich gel coating on the surface of the kaolinite,[37] and a charged layer at the outermost, apical oxygen ions.[38] Furthermore, as aluminum is more soluble than silicon in acid environments,[39] it is possible that natural processes in the soil environment during the formation or weathering of the kaolinite, or acid washing during kaolinite processing, may result in the gibbsite face or edges of the kaolinite crystals being partially depleted of aluminum. Any such preferential removal of aluminum on kaolinite will result in enrichment of silicon on the outer surface of kaolinite. Hence, the high Si/Al ratio may be due to any contribution of these processes and is not resolved at this time.

Structural Changes as a Result of Plasma Treatment. On the basis of results from this work, it can be concluded that the intensity of RF-plasma-induced IR bands is dependent on the period of time used for the treatment and the energy applied, and is independent of the nature of the plasma gas used. The appearance of these IR bands can be associated with changes in bonding with new functional groups being formed in the surface of the kaolinite as a result of the plasma treatment. They appear in regions of the IR spectrum[26] normally associated with hydrogen-bonded OH vibrations (i.e., 3000−3500 cm^{-1}) and CH vibrations (i.e., saturated 2800−3000 cm^{-1}; unsaturated 3000-3200 cm^{-1}). It is not possible to assign the spectrum to specific structures with any certainty due to their breadth, low intensities, and overlap between the different spectral regions.

When Ar^+, the ion used for in-situ sputtering, is also used for the plasma treatment on Georgia kaolin, similar preferential sputtering might be expected to occur although the rate of sputtering may differ.[3,25] In this study, the in-situ ion beam sputtering of kaolinite has resulted in preferential sputtering which distorted the atomic concentration profile, FWHM of major XPS peaks, insulating character (charge shift), and FTIR spectra of structural vibrations of the kaolinite surface relative to that of the original kaolinite. These changes can be used as indicators of surface sputtering and applied to the results of plasma treatment. In general, they show that sputtering has been very limited in all non-Ar plasma treatments. Ar plasma treatment for periods >2 h is necessary to produce changes similar to those found after 3 min of Ar^+-ion-beam etching.

However, whereas extensive surface sputtering occurred in the ion beam in-situ etching and similar new IR bands were formed, their intensities were greatly reduced (almost negligible) relative to plasma treatment for the same period. Therefore, sputtering alone is not the primary mechanism for the formation and accumulation of plasma-induced IR bands on the surface of kaolinite, although it may be an unavoidable or even a necessary part of the process. If the sputtering rate during RF

plasma treatment is assumed to be constant, the rate would be about 1 nm/h (estimated by comparing Si/Al change during depth profiling under high-energy ion beam with RF plasma treatment as a function of the period of plasma treatment). This is about 60 times slower than that determined in the ion beam process. In fact, only the top few layers of kaolinite would be removed after several hours of plasma treatment under the conditions used here.

Sputtering, resulting in ejection of an atom from the surface of the kaolinite to create a dangling bond or active site, may form new surface species in air as soon as the plasma treatment is terminated. However, this process is not likely to explain the formation of the plasma-induced surface functional groups. Ion beam in-situ sputtering on the surface of the kaolinite is far more intensive than that which occurred in RF plasma treatment but the new IR bands on the surface of kaolinite resulting from an ion-beam sputtering process are considerably less intense than those induced as a result of plasma treatment.

These results also show that the plasma-induced functional groups are not likely to be the product of plasma ions chemically reacting with the surface of kaolinite during RF plasma treatment as the number and position of the new bands in the IR spectrum are independent of the nature of the gas used. Another major difference between the plasma-induced reaction and in-situ ion sputtering is the vacuum conditions, i.e., $\sim 10^{-1}$ torr in the plasma and $\sim 10^{-8}$ torr during the ion sputtering.

It is concluded here that the formation of the plasma-induced IR bands is due to some kind of structural and chemical surface modification of kaolinite resulting from reaction between residual hydrocarbon species in the gas phase and surface hydroxyl groups. This conclusion accords with the differences in gas pressures, the independence of plasma gas type, and the IR regions in which the bonds occur. It is also concluded that the energy applied to initiate these physiochemical processes comes from ion (or atom) bombardment, rather than through unactivated chemical reactions between the gas phase and the kaolinite since it is not observed without plasma or ion beam reaction. It is likely that the high-kinetic-energy electrons generated in the plasma and ion impacts may induce this reaction. The ion energies are widely different for the two processes but may also be responsible.

A Comparison of RF Plasma Treatment with Ion Beam Bombardment. The two processes, plasma treatment and ion beam bombardment on kaolinite, not only differ in the concentration of surface functional groups created but also in the changes to the kaolinite surface characteristics such as static charge and surface topography, indicated by peak width changes, in XPS measurement.

(i) Structural Changes. The structural changes in the kaolinite surface clearly involve surface bombardment and possibly surface sputtering processes. The rate of sputtering between the two processes is very different because the ion energy in the two processes is very different. The ion energy in the ion beam process is in the range of 1−3 kV which is far beyond the apparent threshold energy of sputtering, 20−40 eV.[2,3] The ion energy generated in the plasmas is only 0−20 eV. Hence, even the most energetic ion generated in an RF plasma is only just capable of ejecting an atom from the substrate surface explaining why the sputtering yield in the RF plasma process is very low.

As the ion energy generated by the RF plasma process is generally less than the bond energy for most of the bonding in kaolinite, some of the impact energy may be transferred through inelastic collision to lower surface regions or may be converted to heat.[3−6] Although the ion temperature in the RF plasma process is only several-fold higher than ambient temperature, the actual temperature on the surface of the substrate can be much higher. This is because ions are accelerated where the plasma and substrate meet obtaining extra energy in the RF field before hitting the substrate.[1] The surface temperature of the substrate during RF plasma treatment in our conditions may reach more than 200 °C. This would not only enhance atomic vibration in the kaolinite lattice but may also promote solid-state reaction in the surface of the kaolinite.[40] As the etching rate is extremely slow during this process, the surface of the substrate is in a semi-steady state so that surface reconstruction and local amorphisation may both occur as long as the induction time for these surface reactions is feasible. Even when surface sputtering becomes a significant (visible) process, the rate of modification in the surface of the substrate would still be faster than the etching rate.

In ion beam bombardment this would not be the case as the modified surface would be continuously sputtered as soon as new bombardment-induced surface functional groups were created. In addition to the effect of much lower pressure (i.e., residual hydrocarbon concentration), the concentration of new functional groups may not increase due to their continual removal. Both factors severely limit their concentration as observed in the ion-beam-bombardment process.

(ii) Charge Effects. As ion implantation in the surface of an insulating substrate will result in charge buildup of the substrate, the apparent binding energy of the material will be shifted towards a more positive value.[25] Conversely, if there are free electrons or lone pair electrons built up on the surface of an insulating material due to structural or bonding changes, then the apparent binding energy of the insulator will be reduced. The observation of almost no positive surface charge shift on most RF-plasma-treated samples, as determined by XPS measurement, is understandable because ion implantation would be negligible during this process. In contrast, the samples treated up to 2 h in Ar plasma, with no observable sputtering taking place, did show a negative charge shift of around 0.75 eV. This indicates a net surface electron enrichment taking place as a result of the plasma treatment. Although electron trapping is not an inherent property of kaolinite, freed electrons arising from broken bonds due to bombardment, which then become trapped in the lattice of the substrate, may produce this effect. Once the sputtering process of the plasma treatment becomes visible in high--resolution SEM (after 3 h of Ar treatment), it appears that some of the trapped electrons are released, possibly due to a more open structure, causing the charge shift to return to that of the untreated kaolinite although it never reaches that of in-situ sputtered kaolinite.

(iii) Surface Topography. The peak width during XPS measurement is a convolution of several contributions including the natural or inherent width of the core level, the width of the photon source, and the analyzer resolution.[41] Depth resolution in depth profiling is also affected by these instrumental factors, the characteristics of the sample, and fundamental interactions of the ion beam with the sample.[25] As both in-situ ion etching and Ar plasma treatment both involve a sputtering process, although to markedly differing extents, the parameters related to the fundamental interactions of the ion beam with samples may play a major role in affecting the peak width.

During in-situ sputtering, the FWHM of the kaolinite increased in the first 30−60 s and then changed little with further increases in etching time. This type of sputtering-induced effect may be attributed to either micro-topography changes, i.e., the development of surface roughness, or ion implantation. Ion

implantation is less likely because the extent of ion implantation is a function of time and the peak resolution was basically unchanged after the first minute of sputtering. Therefore, it would appear that surface roughness, resulting immediately from sputtering, is the main factor causing the increase in FWHM of the sputtered kaolinite.

If this is the case, then the FWHM value may be used as an indirect measurement to evaluate the extent of surface sputtering. This measurement shows that even after 5 h of plasma treatment (Figure 7), the FWHM of the plasma-treated kaolinite is still less than that of the kaolinite which has undergone 10 min of high-energy ion beam sputtering. Therefore, the surface roughness or damage caused by plasma treatment is very much less than that caused by the in-situ sputtering of the ion beam.

Conclusion

Well-crystallized Georgia kaolin has been modified by RF plasma using varying energy inputs, varying periods of treatment times, and a range of plasma gases. The surface of the modified kaolinite has been studied by XPS and FTIR. New IR absorption bands from the RF-plasma-treated kaolinite are observed at 1407, 2805, 3010, and 3100 cm^{-1}, along with some partially resolved absorption bands occurring near 1440 and 3280 cm^{-1}. The RF plasma treatment on the kaolinite can be defined as a low-energy (<20 eV) ion (or atom) bombardment involving very limited surface sputtering. The formation of new characteristic functional groups on the surface of the kaolinite is generally independent of the nature of the plasma gas. The intensity of these newly formed IR bands is a function of the period of RF plasma treatment and the applied energy. Their intensities are very low (almost negligible) after ion beam sputtering in ultra-high vacuum. The formation of these new bands on the surface of kaolinite is attributed to the changes in bonding associated with surface bombardment (rather than surface sputtering) and reaction between plasma-induced (probably high KE electrons) hydrocarbon species and surface hydroxyl groups.

Acknowledgment. The support of Comalco Research Centre (Dr. Ray Shaw) and an Australian Research Council SPIRT grant for this work is gratefully acknowledged.

References and Notes

(1) Lieberman, M. A.; Lichtenberg, A. J. *Principles of Plasma Discharges and Materials Processing*; John Wiley & Sons, Inc.: New York, 1994.

(2) Mattox, D. M. In *Handbook of Deposition Technologies for Films and Coatings Science, Technologies and Applications*, 2nd ed.; Bunshah, R. F., Ed.; Noyes Publications: Park Ridge, NJ, 1994; p 321.

(3) Winters, H. F. In *Plasma Chemistry III*: Veprek, S., Venugopalan, M., Eds.; Springer-Verlag: New York, 1980; p 69.

(4) Flamm, D. L.; Herb, G. K. In *Plasma Etching—An Introduction*; Manos, D. M., Flamm, D. L., Eds.; Academic Press, Inc.: New York, 1989; p 1.

(5) Boenig, H. V. *Plasma Science and Technology*; Cornell University Press: Ithaca, NY, 1982.

(6) Engel, A. V. *Ionized Gases*; Oxford University Press: New York, 1955.

(7) Brown, N. M. D.; Liu, Z. H. *Appl. Surf. Sci*. **1995**, *90*, 155.

(8) Brown, N. M. D.; Liu, Z. H. *Appl. Surf. Sci*. **1996**, *93*, 89.

(9) Liu, Z. H.; Brown, N. M. D.; McKinley, A. *Appl. Surf. Sci*. **1997**, *108*, 319.

(10) Coen, M. C.; Dietler, G.; Kasas, S.; Groning, P. *Appl. Surf. Sci*. **1997**, *103*, 27.

(11) Tsutsui, K.; Nishizawa, K.; Ikeda, S. *J. Coatings Tech*. **1988**, *60*, 107.

(12) Kobayashi, T.; Kageyama, H.; Kouguchi, K.; Ikeda, S. *J. Coatings Tech*. **1992**, *64*, 41.

(13) Parker, J. L.; Cho, D. L.; Claesson, P. M. *J. Phys. Chem*. **1989**, *93*, 6121.

(14) Parker, J. L.; Claesson, P. M.; Cho, D.; Ahlberg, L.; Tidblad, A. J.; Blomberg, E. *J. Colloid Interface Sci*. **1990**, *134*, 449.

(15) Claesson, P. M.; Cho, D. L.; Golander, C. G.; Kiss, E.; Parker, J. L. *Prog. Colloid Polym. Sci*. **1990**, *82*, 330.

(16) Pitt, W. G. *J. Colloid Interface Sci*. **1989**, *133*, 223.

(17) Kiss, E.; Colander, C-G. *Colloids Surf.* **1990**, *49*, 335.

(18) Smart, R. St. C.; Arora, P. A.; Braggs, B.; Fagerholm, H. M.; Hörr, T. J.; Kehoe, D. C.; Matisons, J. G.; Rosenholm, J. B.; Ralston, J. Modification of oxide, glass, mineral and metal surfaces using adsorption, plasma and sol-gel reactions. In *Interfaces of Ceramic Materials: Impact on Properties and Applications*; Uematsu, K., Moriyoshi, Y., Saito, Y., Nowotny, J., Eds.; Trans. Tech. Publ., 1996; pp 361−404.

(19) Dixon, J. B. *Minerals in Soil Environments*; Dixon, J. B., Weed, S. B., Eds.; SSSA Book Series 1, 2nd ed.; Soil Science Society of America, 1989; p 467.

(20) Hiemstra, T.; deWitt, J. C. M.; van Riemsdijk, W. H. *J. Colloid Interface Sci*. **1989**, *133*, 105.

(21) Murray, H. H. *Appl. Clay Sci.* **1991**, *5*, 379.

(22) Bundy, W. M.; Ishley, J. N. *Appl. Clay Sci.* **1991**, *5*, 374.

(23) Wagner, C. D.; Riggs, W. M.; Davis, L. E.; Moulder, J. F.; Muilenberg, G. E. *Handbook of X-ray photoelectron spectroscopy*; Physical Electronics Division, Perkin-Elmer Corporation, Eden Prairie, 1979.

(24) Seah, M. P.; Swift, P.; Shuttleworth, D. In *Practical Surface Analysis V1— Auger and X-ray photoelectron spectroscopy*, 2nd ed.; Briggs, D., Seah, M. P., Eds.; John Wiley & Sons: New York, 1990; p 541.

(25) Hofmann, S. In *Practical Surface Analysis V1—Auger and X-ray photoelectron spectroscopy*, 2nd ed.; Briggs, D., Seah, M. P., Eds.; John Wiley & Sons: New York, 1990; p 143.

(26) Farmer, V. C. *The Infrared Spectra of Minerals*; Mineralogical Society, London, 1974.

(27) Seah, M. P.; Briggs, D. In *Practical Surface Analysis V1—Auger and X-ray photoelectron spectroscopy*, 2nd ed.; Briggs, D., Seah, M. P., Eds.; John Wiley & Sons: New York, 1990.

(28) Ma, C.; Eggleton, R. A. *Clays Clay Miner.* **1999**, *47*, 181.

(29) Hughes, R. E.; Moore, D. M.; Reynold, R. C., Jr. In *Kaolin Genesis and Utilization*; Murray, H. H., Bundy, W. M., Harvey, C. C., Eds.; Clay Minerals Society, Boulder, Colorado, 1993; p 291.

(30) Kittrick, L. P. *Clays Clay Miner.* **1970**, *18*, 261.

(31) Drever, J. I. *The geochemistry of natural waters*; Prentice Hall: New York, 1988.

(32) van Olphen, H. *An introduction to clay colloid chemistry*, 2nd ed.; John Wiley & Sons, Inc.: New York, 1977.

(33) Braggs, B.; Fornasiero, D.; Ralston, J.; Smart, R. St. *Clays Clay Miner.* **1994**, *42*, 123.

(34) Zhou, Z.; Gunter, W. D. *Clays Clay Miner.* **1992**, *40*, 365.

(35) Tadros, TH. F.; Lyklema, J. *J. Electroanal. Chem*. **1968**, *17*, 267.

(36) Abendroth, R. P. *J. Phys. Chem*. **1972**, *76*, 2547.

(37) Jepson, W. B. *Philos. Trans. R. Soc. London* **1984**, *A 311*, 411.

(38) Gerson, A. R. The surface modification of kaolinite using water vapor plasma. In *Computational Chemistry and Chemical Engineering*; Cisneros, G., Cogorden, J. A., Castro, M., Wang, C., Eds.; World Scientific Publ.: Singapore, 1997; pp 227−235.

(39) Iler, R.K. *The colloid chemistry of silica and silicates*; Cornell. U.P., 1955

(40) Masel, R. I. *Principles of adsorption and reaction on solid surface*; John Wiley & Sons, Inc.: New York, 1996.

(41) Briggs, D.; Riviere, J. C. In *Practical Surface Analysis V1—Auger and X-ray photoelectron spectroscopy*, 2nd ed.; Briggs, D., Seah, M. P., Eds.; John Wiley & Sons: New York, 1990; p 86.